Control of Networked Distributed Energy Resources in Grid-Connected AC Microgrids

Dariush Fooladivanda, Madi Zholbaryssov, and Alejandro D. Domínguez-García

***Abstract*—This paper focuses on the optimal utilization of grid-connected microgrids for providing frequency regulation services to the bulk system they are connected to. We consider microgrids comprised of several distributed energy resources (DER) interconnected via an electrical network. We then formulate a joint DER scheduling and power flow optimization problem in order to determine the DER set-points so that the cost of failing to follow some regulation signal is minimized in each regulation contract; this problem is non-convex. We propose a convex relaxation for this problem, and propose a family of continuous-time control laws, the trajectories of which can be computed in a distributed way. We prove that these converge to an optimal solution of the relaxed problem, and that they result in feasible power flows for the system at each time instant. The proposed continuous-time control laws have to be implemented in a discrete-time fashion over some communication network. We propose a discrete-time approximation of our control laws, and show that the resulting discrete-time control laws converge to an optimal solution of the relaxed problem.**

***Index Terms*—Microgrids, ancillary services, distributed control, sliding mode control.**

I. Introduction

It has been envisioned that future electric power distribution systems will consist of several interconnected microgrids, i.e., small footprint power systems comprising generation and storage resources, distribution assets, and loads [1]-[3]. Microgrids can operate in either grid-connected mode or islanded mode [4]. In islanded mode, the microgrid is disconnected from the rest of the grid, and the objective is to supply electrical power to the customers using the DERs within its footprint [5]. In grid-connected mode, the microgrid optimizes its operation costs by purchasing power from the grid or selling power to the grid. The electrical boundaries of such systems will be precisely defined such that each microgrid can act as a controllable entity with respect to the rest of the grid [6]. Such controllable entities enable the utilization of DERs and flexible loads to participate in electricity markets so as to provide ancillary services, e.g., frequency regulation or reactive power support [1]-[2]. The focus of this paper is the optimal control of microgrids for providing frequency regulation services to the bulk power system when operating in grid-connected mode.

The work presented therein has been partially funded by the U.S. Department of Energy (DOE) within the GEARED Initiative, under grant DE-0006341; the Advanced Research Projects Agency-Energy (ARPA-E) within the NODES program, under Award DE- AR0000695; and by the DOE within the Consortium for Electric Reliability Technology Solutions (CERTS) program.

The authors are with the Department of Electrical and Computer Engineering of the University of Illinois at Urbana-Champaign, Urbana, IL 61801, USA. Email:{dfooladi, zholbar1, aledan}@ILLINOIS.EDU.

Several control strategies have been proposed in the literature in order to mitigate the power fluctuations of non-dispatchable DERs [7]- [9]. These strategies rely on either a grid-following control scheme based on a voltage-sourced converter [10]- [12], or a grid-forming control scheme [13]- [16]. In addition to such local controllers, a microgrid requires an energy management scheme that computes the active and reactive power set-points of its DERs in order to achieve a stable and economic operating point [17]- [26]. In [19], the authors consider a grid-connected microgrid consisting of several generators and loads, propose an algorithm to compute the hourly power outputs of the generators, and provide numerical results for a university campus microgrid in Canada. The authors in [20] propose a control approach for energy management in both grid-connected mode and islanded mode microgrids. This approach consists of two coordinated layers, namely, the schedule layer and the dispatch layer. The schedule layer provides an economic operation scheme based on forecasting data, whereas the dispatch layer provides power of controllable units using real-time data. Finally, the authors numerically demonstrate the performance of their control scheme.

The authors in [21] propose an optimal control strategy for the operation of energy storage in grid-connected microgrids. The proposed controller uses the predicted net energy demand to optimize the operating cost. The authors also propose a robust variation of the controller to handle uncertainty in the prediction of demand and renewable-based generation. Finally, the authors demonstrate the effectiveness of their controller using real data. In [22], the authors propose an energy management system also for grid-connected microgrids with storage. Specifically, they formulate an optimization problem for minimizing the operating cost while maximizing the power provided by the the DERs. They use CPLEX to compute the optimal set-points of the DERs in a centralized fashion. Finally, the authors demonstrate the effectiveness of their system using a real time simulation platform. The authors in [23] propose a consensus algorithm that enables a grid-connected microgrid to compute the set-points of its DERs in a decentralized fashion while ensuring that generation costs are minimized. The authors numerically compare the performance of their algorithm with a centralized method. The authors in [26] consider the energy conversion loss and self-discharge of storage devices in a grid-connected microgrid, and formulate two model predictive control problems. These problems are solved online in order to find an optimal strategy that enables the microgrid to minimize its operation costs in the presence of bounded uncertainties.

Although many approaches in the literature are addressing the energy management problem in grid-connected microgrids, published works do not consider several aspects of energy management, such as the electrical network that connects the DERs, and phase cohesiveness constraints, i.e., the absolute value of the voltage phase angle difference across electrical lines is smaller than $\pi/2$. Therefore, the existing energy management frameworks and control schemes lack performance guarantees when the physical layer undergoes large perturbations.

In this paper, we focus on reducing the cost associated with the failure of a grid-connected microgrid to provide regulation services. More precisely, we consider a network of DERs and loads connected to each other through a set of transmission lines, and assume that the network is connected to the grid through a set of tie-lines. The microgrid operator provides frequency regulation services to the grid by scheduling its DERs and by adjusting the power flows over its tie-lines. We assume that the microgrid operator computed its offer for day-ahead or hour-ahead ancillary service markets, and submitted the offer to the market. The market has been cleared, and the microgrid has received its regulation capacities from the market[1]. To provide regulation services in real-time, the microgrid operator needs to compute the optimal set-points of the DERs (i.e., the active power injections) such that the DERs can meet the regulation demand collectively, and that all the physical constraints within the microgrid are satisfied. To compute the optimal injections, we focus on one single contract, and consider the cost of failing to follow the regulation signals over the contract duration as our objective function. We then formulate a joint DER scheduling and power flow optimization problem (we refer to it as $\mathbf{M}_1$) that enables the microgrid operator to optimize the power flows over the transmission lines as well as the set-points of the DERs such that the cost of failing to follow the regulation signals is minimized over the regulation contract.

Our goal is to optimize the injections of the DERs and the power flows over the transmission lines in a distributed way with some information exchange among different local controllers. To achieve this goal, we follow a three-step procedure. In the first step, we focus on the feasibility set of problem $\mathbf{M}_1$, which is non-convex, and relax the non convex feasible set. We then obtain a convex relaxation of $\mathbf{M}_1$ which we refer to it as $\mathbf{M}_1^{(r)}$. In the second step, we propose a family of control laws that converge to an optimal solution of $\mathbf{M}_1^{(r)}$, and compute feasible power flows and injections for the system at each time instant. Finally, we propose a discrete-time approximation of our continuous-time control laws.

Our contributions are as follows. First, we formulate a joint DER scheduling and power flow optimization problem to optimize the power flows over the lines as well as the set-points of the DERs such that the cost of failing to follow the regulation signals is minimized in each regulation contract; this problem is non-convex. Second, we obtain a convex relaxation of the the proposed problem, and develop a family of continuous-time control laws to compute the optimal power flows over the lines and the optimal set-points of the DERs. These control laws are decentralized, and require some information exchange among different network nodes. Third, we prove that our control laws converge to an optimal solution of the relaxed problem, and that they compute feasible power flows for the system at each time instant. Finally, we numerically show that the proposed discrete-time approximation of our control laws converges to an optimal solution of the relaxed problem.

The reminder of this paper is organized as follows. The system model adopted in this work is introduced in Section II. We formulate the DER scheduling problem, and propose a convex relaxation for this problem in Section III and IV. We then develop a family of control laws for solving the relaxed problem, and show that they converge to an optimal solution of the relaxed problem in Section V and VI. Finally, we numerically demonstrate the effectiveness of our approach in Section VII. All the proofs are presented in an Appendix.

[1]The computation of the microgrid's offer for day-ahead or hour-ahead ancillary service markets is not the subject of this study.

II. Preliminaries

We first introduce the physical (power) layer model of a grid-connected AC microgrid, and then introduce the cyber (communication) layer over which we rely to control the DERs. Finally, we describe the frequency regulation market setting that we are considering in this paper.

A. Physical Layer Model

Consider a microgrid comprised of m generator, n load, and q tie-line buses. Without loss of generality, let $1, 2, \cdots, m$ index the generator buses, and let $m+1, \cdots, m+n$ index the load buses. Each generator bus $i \in \{1 \cdots, m\}$ is connected to either a synchronous generator or an inverter-interfaced power supply, and each load bus $i \in \{m+1 \cdots, m+n\}$ is connected to either a controllable load or an uncontrollable load. We assume that the microgrid is operating in grid-connected mode, and that it is connected to the bulk system via q tie-lines; let $m+n+1, \cdots, m+n+q$ index the corresponding tie-line buses. Further, we assume that the network interconnecting the generator, load, and tie-line buses is lossless and inductive so that it can be represented by the admittance matrix $\mathbf{Y}$. When electrical lines in the microgrid are lossy, but with sufficiently uniform resistance-to-reactance ratios, the lossless model can be still recovered through a linear transformation (see, e.g., [30]).

The topology of the microgrid can be represented by an undirected graph, $\mathcal{G}(\mathcal{N}, \mathcal{E})$, where $\mathcal{N} = \mathcal{N}^{(G)} \cup \mathcal{N}^{(L)} \cup \mathcal{N}^{(T)}$, with each $i \in \mathcal{N}^{(G)} = \{1, \cdots, m\}$ corresponding to a generator bus, each $i \in \mathcal{N}^{(L)} = \{m+1, \cdots, m+n\}$ corresponding to a load bus, and each $i \in \mathcal{N}^{(T)} = \{m+n+1, \cdots, m+n+q\}$ corresponding to a tie-line bus; and where each element in the edge set $\mathcal{E} = \{e_1, \cdots, e_{|\mathcal{E}|}\}$ corresponds to a transmission line connecting a pair of buses. Let $e_a = (i, j)$ be an unordered pair of vertices indicating that edge e_a is incident to vertices i and j, and let M denote a node-to-edge incidence matrix for graph $\mathcal{G}(\mathcal{N}, \mathcal{E})$. To obtain a node-to-edge incidence matrix for undirected graph $\mathcal{G}(\mathcal{N}, \mathcal{E})$, we first apply an arbitrary orientation to the edges. Given such orientation, the incidence matrix $M \in \mathbb{R}^{|\mathcal{N}|\times|\mathcal{E}|}$ has the following form:

$$M = [m_{ia}],\ i = 1, \cdots, |\mathcal{N}|,\ a = 1, \cdots, |\mathcal{E}|, \tag{1}$$

where

$$m_{ia} = \begin{cases} 1, \text{ edge } e_a \text{ is incident from vertex } i, \\ -1, \text{ edge } e_a \text{ is incident to vertex } i, \\ 0, \text{ otherwise.} \end{cases} \tag{2}$$

With respect to an arbitrarily chosen spanning tree of the graph $\mathcal{G}$, an edge, which does not belong to the spanning tree, and the path in the spanning tree between the vertices of the edge form a cycle. Such cycles are referred to as fundamental cycles (see [27, p. 27]). There are $|\mathcal{E}| - |\mathcal{N}| + 1$ fundamental cycles, since there are $|\mathcal{E}| - |\mathcal{N}| + 1$ edges, which do not belong to the spanning tree. We denote the fundamental cycles by $\mathcal{C}_i(\mathcal{N}_i, \mathcal{E}_i)$, $i = 1, \ldots, |\mathcal{E}| - |\mathcal{N}| + 1$, where $\mathcal{N}_i$ and $\mathcal{E}_i$ are the sets of vertices and edges of $\mathcal{C}_i$, respectively.

We also define the entries of the fundamental cycle matrix, denoted by $N \in \mathbb{R}^{(|\mathcal{E}|-|\mathcal{N}|+1)\times|\mathcal{E}|}$, as follows:

$$N = [n_{ia}],\ i = 1, \cdots, |\mathcal{E}| - |\mathcal{N}| + 1,\ a = 1, \cdots, |\mathcal{E}|, \tag{3}$$

where

$$n_{ia} = \begin{cases} 1 & \text{if } e_a \in \mathcal{E}_i, \exists j : m_{ja} = 1, \\ -1 & \text{if } e_a \in \mathcal{E}_i, \exists j : m_{ja} = -1, \\ 0 & \text{otherwise.} \end{cases} \tag{4}$$

Let us assume that time is divided into slots of length T. At each time slot k, there are three types of active power injections into the microgrid. Let $g_i[k]$ denote the active power generated by the generator at bus $i \in \mathcal{N}^{(G)}$, $\ell_i[k] \geq 0$ denote the load at load bus $i \in \mathcal{N}^{(L)}$ at time slot k, and $p_i[k]$ denote the active power injection through the tie-line connected to bus $i \in \mathcal{N}^{(T)}$ at time slot k. Recall that we are considering only fast-following DERs, i.e., generators and flexible loads with fast ramping rates. Hence, we can ignore their fast time-scale dynamics in the physical layer model, and model each DER via its upper and lower power injection limits. More precisely, we consider the following constraint on the active power injection at each generator bus $i \in \mathcal{N}^{(G)}$:

$$\underline{g}_i[k] \leq g_i[k] \leq \overline{g}_i[k], \quad \forall k, \tag{5}$$

where the lower bound $\underline{g}_i[k]$ is non-negative. Similarly, we consider the following constraint on the load at each load bus $i \in \mathcal{N}^{(L)}$:

$$\underline{\ell}_i[k] \leq \ell_i[k] \leq \overline{\ell}_i[k], \quad \forall k\ . \tag{6}$$

Note that we will have $\underline{\ell}_i[k] = \overline{\ell}_i[k]$ at time slot k if the load at bus $i \in \mathcal{N}^{(L)}$ is uncontrollable at time slot k.

The upper and lower limits on the DERs can be stochastic for some DERs (e.g., renewable resources and flexible loads). Later, we will mention that the independent system operator (ISO) sends regulation signals to the microgrid every 2 to 4 s, and that the time slot duration T is in the order of 1 millisecond. Let us assume that the ISO sends regulation signals to the microgrid every $W \in \mathbb{Z}^+$ time slots. It is reasonable to assume that the upper and lower bounds on $g_i[k]$'s and $\ell_i[k]$'s are constant over time periods which are less than W time slots. Because of this, we make the following assumptions:

1) The microgrid operator can perfectly estimate $\underline{g}_i[k]$'s, $\overline{g}_i[k]$'s, $\underline{\ell}_i[k]$'s, and $\overline{\ell}_i[k]$'s at least W time slots beforehand.
2) The values of the upper and lower bounds $\underline{g}_i[k]$'s, $\overline{g}_i[k]$'s, $\underline{\ell}_i[k]$'s, and $\overline{\ell}_i[k]$'s are quasi-static in the sense that these values are constant over time periods which are less than W time slots.

Under the assumptions above, each local controller in the microgrid only needs to estimate $\underline{g}_i[k]$'s, $\overline{g}_i[k]$'s, $\underline{\ell}_i[k]$'s, and $\overline{\ell}_i[k]$'s every W time slots since the upper and lower bounds are constant over time periods which are less than W time slots.

As mentioned earlier, $p_i[k]$ denotes the active power injection through the tie-line connected to bus $i \in \mathcal{N}^{(T)}$ at time slot k. If $p_i[k] < 0$, the bulk system supplies power during time slot k; whereas it draws power from the grid if $p_i[k] > 0$. The active power injections into the bulk grid, i.e., the $p_i[k]$'s are limited by the thermal limits on the corresponding tie-lines. We consider the following constraint on the active power injection $p_i[k]$ at each tie-line bus $i \in \mathcal{N}^{(T)}$:

$$\underline{p}_i \leq p_i[k] \leq \overline{p}_i, \quad \forall k, \tag{7}$$

where $\underline{p}_i$ and $\overline{p}_i$ denote the minimum and maximum allowable power flows on the tie-line connected to bus $i \in \mathcal{N}^{(T)}$, respectively. To model the active power injections at bus $i \in \mathcal{N}^{(T)}$, let $p_i^0[k]$ denote the scheduled tie-line power flow for the tie-line connected to bus i at time slots k. Here, we refer to $p_i^0[k]$ as the nominal power exchange for the tie-line connected to bus i at time slots k. At each time slot k, the active power injection at bus i equals $(p_i^0[k] + \Delta p_i[k])$, where $\Delta p_i[k]$ denotes the difference between the actual active powe r injection at bus i and the nominal power exchange for the tie-line connected to bus i at time slots k. Note that the microgrid operator offers some nominal power exchange for each one of its tie-lines in the energy market, and that the final values are determined by the ISO. Therefore, at each time slot k, the values of $p_i^0[k]$'s are fixed and known to the microgid operator.

Let $V_i[k]$ and $\theta_i[k]$ denote the voltage magnitude and phase angle of bus $i \in \mathcal{N}$, respectively, at time slot k. The net active power injected into the network at node i equals $\sum_{j\in\mathcal{N}} V_i[k]V_j[k]B_{ij}\ \sin(\theta_i[k] - \theta_j[k])$. By using the node-to-edge incidence matrix M, the net active power injections can be represented by

$$\begin{bmatrix} g[k] \\ -\ell[k] \\ -p[k] \end{bmatrix} = Mf[k], \quad \forall k, \tag{8}$$

$$p[k] = p^0[k] + \Delta p[k], \quad \forall k, \tag{9}$$

where

$$g[k] = [g_1[k], \cdots, g_m[k]]^{\mathrm{T}}, \tag{10}$$

$$\ell[k] = [\ell_{m+1}[k], \cdots, \ell_{m+n}[k]]^{\mathrm{T}}, \tag{11}$$

$$\Delta p[k] = [\Delta p_{m+n+1}[k], \cdots, \Delta p_{m+n+q}[k]]^{\mathrm{T}}, \tag{12}$$

$$p^0[k] = [p^0_{m+n+1}[k], \cdots, p^0_{m+n+q}[k]]^{\mathrm{T}}, \tag{13}$$

$$p[k] = [p_{m+n+1}[k], \cdots, p_{m+n+q}[k]]^{\mathrm{T}}, \quad (14)$$

$$f[k] = [f_1[k], \cdots, f_{|\mathcal{E}|}[k]]^{\mathrm{T}} \ . \quad (15)$$

Given edge $e_a = (i,j)$, line flow $f_a[k]$ equals $\gamma_a[k]\sin(\theta_i[k]-\theta_j[k])$, where $\gamma_a[k] = V_i[k]V_j[k]B_{ij}$ and $B_{ij} = -b_{ij}$ with $b_{ij} < 0$ denoting the susceptance of the line connecting nodes i and j. Since the controllers that we propose later operate at the time scale of the secondary frequency controller, the voltage dynamics governed by the voltage droop controllers can be ignored without jeopardizing the model accuracy (see, e.g., [29, Section III-C, pp. 826-827]); thus, in this paper, we do not consider the reactive power models for generators and loads, and assume that voltage magnitudes $V_i[k]$'s are constant.

Power flows $f_a[k]$'s are limited by thermal limit constraints. To capture such constraints, let $\underline{f}_a$ and $\overline{f}_a$ denote the minimum and maximum allowable power flows on the line interconnecting nodes i and j, respectively, at time slot k. Given edge $e_a = (i,j)$, we consider the following constraint on power flow $f_a[k]$:

$$\underline{f}_a \leq f_a[k] \leq \overline{f}_a, \quad \forall k. \quad (16)$$

Note that the values of the parameters $\underline{f}_a$'s and $\overline{f}_a$'s can be computed in advance for all $a \in \{1, \cdots, |\mathcal{E}|\}$.

B. Cyber Layer Model

Each bus i is equipped with a local controller, transceiver, and measurement device which allow bus i to exchange information with the local controllers of other buses as well as the DER connected to bus i if there is any. In addition, each DER connected to bus i is equipped with a local controller and receiver through which information can be received from the local controller of bus i. The transceivers and receivers are connected through a communication network which sends the feedback information to different nodes. We assume that the transceiver at bus i only transmits the feedback information of bus i to the neighbours of bus i in graph $\mathcal{G}(\mathcal{N}, \mathcal{E})$, and that the communication network has the same topology as the physical layer network. In Section V and VI, we will propose a set of distributed control laws implemented over the cyber layer. The combination of the proposed control laws and the cyber layer enables the microgrid operator to control the DERs in a distributed way. When the communication network is directed, we only need to select the orientation of the edges according to the direction of our communication network. We can then use the control laws and convergence results proposed in Section V and VI to compute the set-points of the DERs.

C. Frequency Regulation Market Mechanism

The microgrid offers frequency regulation services to the ISO in the corresponding market. A risk-neutral microgrid will attempt to maximize its expected profits over the contract period. Without loss of generality, we assume that the duration of the contract is $D = KT$, and hence every K time slots, a new regulation contract starts. The microgrid's revenue maximization problem can be cast as a stochastic control problem. Typically, characterizing an optimal causal control policy in stochastic control problems is challenging. For simplicity, the microgrid operator first selects a set of simple control policies for its DERs in order to compute their response to the regulation signals sent by the ISO. This set of control policies will determine how the microgrid will respond to the regulation signals sent by the ISO. Given the control policies and generation capacity limits of the DERs, the microgrid operator computes its energy and regulation offers, and participates in the market. When the market is cleared, the microgrid operator receives its regulation capacity, as well as the amount of energy that should be provided through the tie-lines. Now, the microgrid operator needs to schedule its DERs so that they collectively follow the regulation signal sent by the ISO; i.e., the problem is to disaggregate the regulation signal to be followed among the DERs within the microgrid.

In this paper, we assume that the microgrid operator computed its offer for day-ahead or hour-ahead regulation service markets, and submitted the offer to the market. We further assume that the market has been cleared, and the microgrid has been selected to provide up and down regulation services, with the cleared up and down regulation capacities being respectively $\overline{r}_i$'s and $\underline{r}_i$'s that can be provided by the microgrid through its tie-line. The computation of the microgrid's offer for day-ahead or hour-ahead ancillary service markets is not the subject of this the paper, but how to solve the disaggregation problem in a distributed fashion.

Let $\underline{r}_i$ and $\overline{r}_i$ denote the maximum downward and upward regulations respectively, that can be provided through the tie-line connected to bus $i \in \mathcal{N}^{(T)}$. Given the $\underline{r}_i$'s and $\overline{r}_i$'s, the values of $\underline{r}$ and $\overline{r}$ can be obtained as follows:

$$\overline{r} = \sum_{i \in \mathcal{N}^{(T)}} \overline{r}_i, \quad \text{and} \quad \underline{r} = \sum_{i \in \mathcal{N}^{(T)}} \underline{r}_i \ .$$

The computation of the $\underline{r}_i$'s and $\overline{r}_i$'s is not the subject of this work, and assume that they are computed beforehand.

At the beginning of each contract, the microgrid operator and ISO agree on the regulation parameters $\underline{r}$ and $\overline{r}$ (in pu) for the contract duration $D = KT$. The ISO sends regulation signals to the microgrid every W time slots, and commits that the regulation signal $r[k_0]$ in time slot $k_0 \in \mathcal{K}$ where $\mathcal{K} = \{k \in \mathbb{Z}^+ | \mathrm{mod}(k-1, W) = 0, \ k \leq K\}$, will satisfy the following constraint:

$$\underline{r} \leq r[k_0] \leq \overline{r} \ .$$

There is no other constraint on the regulation signals sent by the ISO. The microgrid must supply constant power $r[k_0]$ during the next W time slots if $r[k_0]$ is positive, and draw constant power $r[k_0]$ from the grid during the next W time slots if it is negative. For all $k \in \{k_0, \cdots, k_0 + W - 1\}$, we define $r[k]$ to be equal to $r[k_0]$. The time scales that we are using in this study, are illustrated in Fig. 1.

The microgrid is rewarded for the amount of energy that it effectively supplies or draws during the contract, and is penalized for any failure in responding to the regulation signals sent by the ISO. Therefore, the microgrid can maximize its net revenue by minimizing the cost of failing to follow the

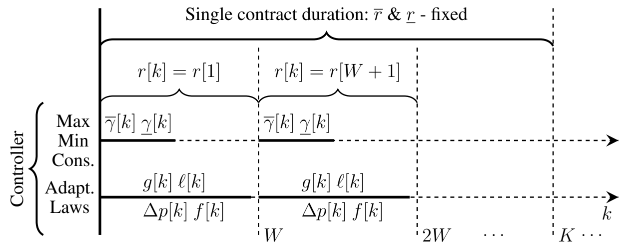

Fig. 1. Timeline of distributed implementation of the proposed controller.

regulation signals over the contract period $D = KT$. At each time slot k, the microgrid operator divides the regulation signal $r[k]$ between its tie-lines according to their capacities (i.e., $\underline{r}_i$'s and $\overline{r}_i$'s) as follows:

$$r_i[k] = r[k]\left(\frac{\underline{r}_i}{\underline{r}}\mathbf{1}_{r[k]<0} + \frac{\overline{r}_i}{\overline{r}}\mathbf{1}_{r[k]>0}\right),\ \forall i \in \mathcal{N}^{(T)};$$

hence, the amount of regulation failure in each tie-line $i \in \mathcal{N}^{(T)}$ at time slot k equals $(\Delta p_i[k] - r_i[k])$.

We assume that at each time slot k, the cost of failing to follow some regulation signal in tie-line $i \in \mathcal{N}^{(T)}$ is quadratically proportional to the imbalance $(\Delta p_i[k] - r_i[k])$. Under this assumption, the cost of failing to follow the regulation signals can be computed by

$$C(\Delta p) = \sum_{k=1}^{K}\sum_{i\in\mathcal{N}^{(T)}} \zeta[k]\left(\Delta p_i[k] - r_i[k]\right)^2, \quad \text{(in \$)}$$

where $\zeta[k]$ is a stochastic price parameter ($\$/\text{Watt}^2$) modeling the price of purchasing or selling electricity at time slot k (i.e., the price of electricity in the real-time energy market). Note that we do not necessarily need to select a quadratic cost function. We only need to ensure that the cost function is smooth, convex, and separable in its arguments. For such cost functions, with a slight modification in our results in Section V, we can propose a new set of adaptation laws to compute the set-points of the DERs.

The cost function $C(\Delta p)$ is stochastic since it is a function of stochastic parameters $r[k]$'s and $\zeta[k]$'s. However, there is no coupling across time among the physical constraints in the microgrid. Hence, the cost of failing to follow the regulation signals can be minimized in an online setting in which at the beginning of each time slot k, the realizations of the stochastic parameters $r[k]$ and $\zeta[k]$ are revealed to the microgrid operator. Next, we focus on a single contract, and formulate the problem of controlling the DERs over the contract duration $D = KT$.

III. Problem Statement

Consider a single frequency regulation contract. The microgrid operator aims at minimizing the cost of failing to follow some regulation signal over the contract duration $D = KT$ while ensuring that all the physical constraints are satisfied. Recall that the regulation signals and electricity prices, $r[k]$'s and $\zeta[k]$'s, respectively, are stochastic, and that there is no coupling across time among the physical constraints. In addition, the ISO sends regulation signals every W time slots. Therefore, we can minimize the cost of failing to follow some regulation signal over the contract duration $D = KT$ by computing a solution to the following problem at each time slot $k \in \mathcal{K}$. Given the parameters M, N, $\underline{g}_i[k]$, $\overline{g}_i[k]$, $\underline{\ell}_i[k]$, $\overline{\ell}_i[k]$, $\underline{f}_a$, $\overline{f}_a$, $p^0[k]$, $\overline{p}_i$, and $\underline{p}_i$, compute $f[k]$, $g[k]$, $\ell[k]$, $p[k]$, and $\Delta p[k]$, so as to minimize the following objective function:

$$\mathbf{M}_1: \min_{f,g,\ell,p,\Delta p} \sum_{i\in\mathcal{N}^{(T)}} \zeta[k]\left(\Delta p_i[k] - r_i[k]\right)^2$$

$$\text{subject to} \begin{bmatrix} g[k] \\ -\ell[k] \\ -p[k] \end{bmatrix} = Mf[k], \tag{17}$$

$$p[k] = p^0[k] + \Delta p[k], \tag{18}$$

$$\underline{p}_i \le p_i[k] \le \overline{p}_i, \quad \forall i \in \mathcal{N}^{(T)}, \tag{19}$$

$$\underline{g}_i[k] \le g_i[k] \le \overline{g}_i[k], \quad \forall i \in \mathcal{N}^{(G)}, \tag{20}$$

$$\underline{\ell}_i[k] \le \ell_i[k] \le \overline{\ell}_i[k], \quad \forall i \in \mathcal{N}^{(L)}, \tag{21}$$

$$\underline{f}_a \le f_a[k] \le \overline{f}_a, \quad \forall e_a \in \mathcal{E}, \tag{22}$$

$$N\ \arcsin(\Gamma^{-1}[k]f[k]) = 0, \tag{23}$$

where $\Gamma[k] = \text{diag}(\gamma_1[k], \cdots, \gamma_{|\mathcal{E}|}[k])$. The constraint in (23) ensures that at time slot $k \in \mathcal{K}$, the voltage phase angles satisfy the following cycle constraint:

$$\sum_{(i,j)\in\mathcal{E}_c} (\theta_i[k] - \theta_j[k]) = 0,$$

for each fundamental cycle $\mathcal{C}_c(\mathcal{N}_c, \mathcal{E}_c)$.

It is hard to solve $\mathbf{M}_1$ since the cycle constraint in (23) is non-convex. Our goal is to obtain decision-making policies that enable us to use information available at each time slot $k \in \mathcal{K}$ to compute sub-optimal solutions to $\mathbf{M}_1$; to do so, we follow a three-step procedure. First, in Section IV, we focus on the feasibility region of $\mathbf{M}_1$, and approximate the non-convex constraint (23) with a set of linear inequality constraints. We then propose a relaxation (we refer to it as $\mathbf{M}_1^{(r)}$) for $\mathbf{M}_1$, and discuss the conditions under which the proposed relaxation is exact. Second, in Section V, we propose a set of decentralized control laws that enable us to compute an optimal solution to the proposed relaxation. Finally, we propose a discrete-time approximation of our control laws.

IV. Feasible Set and Relaxation

Problem $\mathbf{M}_1$ is non-convex due to the cycle constraint in (23). We first use the technique proposed in [25] to obtain a convex inner approximation of the constraint set of $\mathbf{M}_1$, and then propose a convex relaxation to $\mathbf{M}_1$.

A. Inner Approximation

In [25], the authors propose convex inner approximations to non-convex cycle constraint in flow networks. In particular, they focus on electrical networks, and propose a convex inner approximation to the cycle constraint in (23). They show that a convex inner approximation to constraint (23) can be obtained by adjusting the upper and lower limits of the flows along the edges of the cycles. More precisely, we can approximate the cycle constraint in (23) with a set of box constraints as follows:

$$\underline{f}_a + \mu_i[k] \leq f_a[k],\ \forall k,\ \forall e_a \in \mathcal{E}_i,\ \forall i \in \mathcal{L}, \quad (24)$$

$$\underline{f}_a + \mu_{i_1}[k] + \mu_{i_2}[k] \leq f_a[k],\ \forall k,\ \forall e_a \in \mathcal{E}_{i_1} \cap \mathcal{E}_{i_2},\ \forall i_1, i_2 \in \mathcal{L}, i_1 \neq i_2, \quad (25)$$

$$f_a[k] \leq \overline{f}_a - \mu_i[k],\ \forall k,\ \forall e_a \in \mathcal{E}_i,\ \forall i \in \mathcal{L}, \quad (26)$$

$$f_a[k] \leq \overline{f}_a - \mu_{i_1}[k] - \mu_{i_2}[k],\ \forall k,\ \forall e_a \in \mathcal{E}_{i_1} \cap \mathcal{E}_{i_2},\ \forall i_1, i_2 \in \mathcal{L}, i_1 \neq i_2, \quad (27)$$

where $\mathcal{L} = \{1, \cdots, |\mathcal{E}| - |\mathcal{N}| + 1\}$, and

$$\mu_i[k] = \frac{\overline{\gamma}_i[k]}{2} + \frac{\underline{\gamma}_i[k]}{2} \sin\left(\frac{\pi/2}{|\mathcal{E}_i| - 1}\right), \quad (28)$$

with

$$\overline{\gamma}_i[k] = \max_{e_j \in \mathcal{E}_i} \gamma_j[k] \quad \text{and} \quad \underline{\gamma}_i[k] = \min_{e_j \in \mathcal{E}_i} \gamma_j[k].$$

Note that the values of the parameters $\overline{\gamma}_i[k]$'s and $\underline{\gamma}_i[k]$'s can be pre-computed distributively by each node of cycle $\mathcal{C}_i$ using the so-called max- and min-consensus algorithms (see, e.g., [24]).

We now explain how each node along cycle $\mathcal{C}_i$ can compute the value of the parameters $\mu_i[k]$. To do so, each node of cycle $\mathcal{C}_i$ can obtain the values of the parameters $\overline{\gamma}_i[k]$ and $\underline{\gamma}_i[k]$ distributively by using max- and min-consensus algorithms. Each node $j \in \mathcal{N}_i$ maintains local estimates for $\overline{\gamma}_i$ and $\underline{\gamma}_i$, denoted by $\psi_j[k]$ and $\chi_j[k]$, respectively, at iteration k, and transmits them to its neighbors at each iteration. Both estimates are initialized so that $\psi_j[0] = \max\{\gamma_a[0], \gamma_b[0]\}$ and $\chi_j[0] = \min\{\gamma_a[0], \gamma_b[0]\}$, where e_a and e_b are incident at node j and belong to $\mathcal{E}_i$; then, at each iteration k, the estimates are updated by

$$\psi_j[k+1] = \max_{(l,j) \in \mathcal{E}_i \cup (j,j)} \psi_l[k], \quad (29)$$

$$\chi_j[k+1] = \min_{(l,j) \in \mathcal{E}_i \cup (j,j)} \chi_l[k]. \quad (30)$$

As shown in [24], after a finite number of iterations, (29) – (30) converge to $\overline{\gamma}_i[k]$ and $\underline{\gamma}_i[k]$, respectively.

This convex inner approximation technique enables us to compute either exact or high quality solutions to $\mathbf{M}_1$. This inner approximation is exact if the network's topology is a tree. When the proposed relaxation is not exact, we can obtain more accurate convex inner approximations by using linear constraints. However, the use of box constraints is the simplest way to convexify the cycle constraints distributively since even alternative linear constraints cannot necessarily be implemented in a distributive manner. For more information on the inner approximation technique, we refer the reader to [25].

B. *Convex Relaxation*

We now propose a convex relaxation to $\mathbf{M}_1$ as follows:

$$\mathbf{M}_1^{(r)} : \min_{f,g,\ell,p,\Delta p} \sum_{i \in \mathcal{N}^{(T)}} (\Delta p_i[k] - r_i[k])^2$$
$$\text{subject to} \quad (17) - (21),$$
$$\underline{F}_a[k] \leq f_a[k] \leq \overline{F}_a[k],\ \forall e_a \in \mathcal{E}, \quad (31)$$

with

$$\underline{F}_a[k] = \max\left\{\underline{f}_a, \max_{(i_1,i_2) \in \mathcal{L}_2(e_a)} \{\underline{f}_a + \mu_{i_1}[k] + \mu_{i_2}[k]\}, \max_{i \in \mathcal{L}_1(e_a)} \{\underline{f}_a + \mu_i[k]\}\right\}, \quad (32)$$

$$\overline{F}_a[k] = \min\left\{\overline{f}_a, \min_{(i_1,i_2) \in \mathcal{L}_2(e_a)} \{\overline{f}_a - \mu_{i_1}[k] - \mu_{i_2}[k]\}, \min_{i \in \mathcal{L}_1(e_a)} \{\overline{f}_a - \mu_i[k]\}\right\}, \quad (33)$$

where $\mathcal{L}_2(e_a) = \{(i_1, i_2) | i_1, i_2 \in \mathcal{L},\ i_1 \neq i_2,\ e_a \in \mathcal{E}_{i_1} \cap \mathcal{E}_{i_2}\}$ and $\mathcal{L}_1(e_a) = \{i | i \in \mathcal{L},\ e_a \in \mathcal{E}_i\}$. The values of the parameters $\underline{F}_a[k]$'s and $\overline{F}_a[k]$'s can be computed beforehand. We have omitted the term $\zeta[k]$ from the objective function in $\mathbf{M}_1^{(r)}$ since the value of $\zeta[k]$ is revealed to the microgrid operator at the beginning of time slot k. The proposed relaxation is a convex quadratic program which can be solved efficiently.

Our objective is to obtain a set of decentralized control laws that allows the microgrid operator to compute the optimal set-points of its DERs in a distributed fashion. To do so, in Section V, we propose a set of continuous-time control laws that enable us to compute an optimal solution of $\mathbf{M}_1^{(r)}$ in a distributed fashion. Then, in Section VI, we discretize the proposed control laws, and propose a discrete-time version that converge to an optimal solution of $\mathbf{M}_1^{(r)}$.

V. A Set of Decentralized Control Laws

We now present a set of continuous-time control laws that converge to an optimal solution of $\mathbf{M}_1^{(r)}$. For simplicity, we omit the notion of time slot (i.e., k), and introduce the notion of time t where $t \in [(k-1)T, (k+W-1)T]$, with $k \in \mathcal{K} = \{k \in \mathbb{Z}^+ | \text{mod}(k-1, W) = 0,\ k \leq K\}$. Recall that the ISO sends regulation signals every W time slots, and hence the microgrid operator needs to compute a new set of set-points for its DERs in time period $[(k-1)T, (k+W-1)T]$.

A. *Control Laws for Generators*

Consider generator bus $i \in \mathcal{N}^{(G)}$, and let the following control law to be implemented by the generator at bus i:

$$\frac{d}{dt} g_i(t) = \underline{\alpha}_i \underline{u}_i^{(g)}(t) - \overline{\alpha}_i \overline{u}_i^{(g)}(t) - \beta_i u_i(t), \quad (34)$$

with

$$\underline{u}_i^{(g)}(t) = \begin{cases} 0, & \text{if } g_i(t) > \underline{g}_i, \\ 1, & \text{if } g_i(t) < \underline{g}_i, \end{cases} \quad (35)$$

$$\overline{u}_i^{(g)}(t) = \begin{cases} 1, & \text{if } g_i(t) > \overline{g}_i, \\ 0, & \text{if } g_i(t) < \overline{g}_i, \end{cases} \quad (36)$$

$$u_i(t) = \begin{cases} 1, & \text{if } w_i(t) > \sum_{e \in \mathcal{N}_i^+} f_e(t) - \sum_{e \in \mathcal{N}_i^-} f_e(t), \\ -1, & \text{if } w_i(t) < \sum_{e \in \mathcal{N}_i^+} f_e(t) - \sum_{e \in \mathcal{N}_i^-} f_e(t), \end{cases} \quad (37)$$

$$w_i(t) = \begin{cases} g_i(t), & \text{if } i \in \mathcal{N}^{(G)}, \\ -\ell_i(t), & \text{if } i \in \mathcal{N}^{(L)}, \\ -(p_i^0(t) + \Delta p_i(t)), & \text{if } i \in \mathcal{N}^{(T)}, \end{cases} \quad (38)$$

where $p_i^0(t) = p_i^0[k]$ for all $t \in [(k-1)T, (k+W-1)T]$ since the amount of power transfer $p_i^0[k]$ is fixed over the time period $[(k-1)T, (k+W-1)T]$. $\mathcal{N}_i^+$ (respectively $\mathcal{N}_i^-$) denotes the set of outgoing lines (respectively incoming lines) of bus i excluding the tie-lines if there is any tie-line connected to bus i. These sets are determined by the node-to-edge incidence matrix M.

B. Control Laws for Loads

Consider load bus $i \in \mathcal{N}^{(L)}$, and let the following control law to be implemented by the load at bus i:

$$\frac{d}{dt}\ell_i(t) = \underline{\alpha}_i \underline{u}_i^{(\ell)}(t) - \overline{\alpha}_i \overline{u}_i^{(\ell)}(t) + \beta_i u_i(t), \tag{39}$$

where

$$\underline{u}_i^{(\ell)}(t) = \begin{cases} 0, & \text{if } \ell_i(t) > \underline{\ell}_i, \\ 1, & \text{if } \ell_i(t) < \underline{\ell}_i, \end{cases} \tag{40}$$

$$\overline{u}_i^{(\ell)}(t) = \begin{cases} 1, & \text{if } \ell_i(t) > \overline{\ell}_i, \\ 0, & \text{if } \ell_i(t) < \overline{\ell}_i, \end{cases} \tag{41}$$

C. Control Laws for Tie-lines

Consider tie-line bus $i \in \mathcal{N}^{(T)}$, and let the following control law to be implemented by the tie-line $e_a = (i,j)$ connected to bus i:

$$\begin{aligned}\frac{d}{dt}\Delta p_i(t) = &- 2\left(\Delta p_i(t) - r_i(t)\right) + \beta_i u_i(t) \\ &+ \underline{\alpha}_{i,j}\underline{u}_{i,j}(t) - \overline{\alpha}_{i,j}\overline{u}_{i,j}(t),\end{aligned} \tag{42}$$

where

$$\underline{u}_{i,j}(t) = \begin{cases} 0, & \text{if } p_i(t) > \underline{f}_a, \\ 1, & \text{if } p_i(t) < \underline{f}_a, \end{cases} \tag{43}$$

$$\overline{u}_{i,j}(t) = \begin{cases} 1, & \text{if } p_i(t) > \overline{f}_a, \\ 0, & \text{if } p_i(t) < \overline{f}_a, \end{cases} \tag{44}$$

Note that $r_i(t) = r_i[k]$ for all $t \in [(k-1)T, (k+W-1)T]$ since the regulation signal $r_i[k]$ is fixed over the time period $[(k-1)T, (k+W-1)T]$. Here, we assume that the ISO controls the load bus j. Hence, we do not consider the flow conservation constraint at bus j in (42).

D. Control Laws for Line Flows

Consider bus $i \in \mathcal{N}$, and let the following control law to be implemented by the outgoing edge $e_a = (i,j)$ of bus i:

$$\frac{d}{dt}f_a(t) = \underline{\alpha}_{i,j}\underline{u}_{i,j}(t) - \overline{\alpha}_{i,j}\overline{u}_{i,j}(t) + \beta_i u_i(t) - \beta_j u_j(t), \tag{45}$$

where

$$\underline{u}_{i,j}(t) = \begin{cases} 0, & \text{if } f_a(t) > \underline{F}_a, \\ 1, & \text{if } f_a(t) < \underline{F}_a, \end{cases} \tag{46}$$

$$\overline{u}_{i,j}(t) = \begin{cases} 1, & \text{if } f_a(t) > \overline{F}_a, \\ 0, & \text{if } f_a(t) < \overline{F}_a, \end{cases} \tag{47}$$

Our control laws in (34)-(47) enable the microgrid operator to compute the optimal set-point of each DER in a distributed fashion. More precisely, the measurement device at each bus i measures the incoming flows to bus i, and the local controller at bus i computes the outgoing power flows using the control laws in (42) and (45). Then, using the received measurements and the computed power flows, the local controller at bus i computes some feedback information, using (37) and (38), to be sent to the neighbors of bus i. Using the feedback information $u_i(t)$, the DERs compute their set-points using their control laws which are either (34) or (39).

In (34)-(47), $s_i(t)$, $s_a^e(t)$, $\underline{\alpha}_i$, $\overline{\alpha}_i$, $\underline{\alpha}_{i,j}$, $\overline{\alpha}_{i,j}$, and β_i are the design parameters which can affect convergenc. The following theorem provides a set of sufficient conditions under which the proposed control laws converge to the optimal solution of $\mathbf{M}_1^{(r)}$. The proof is provided in the appendix.

Theorem 1. *Given $r_i[k]$'s, $p_i^0[k]$'s, $\underline{p}_i$'s, and $\overline{p}_i$'s, let $\alpha = \underline{\alpha}_{i,j} = \overline{\alpha}_{i,j} = \underline{\alpha}_i = \overline{\alpha}_i$, and $\beta = \beta_i$ be constants satisfying the following inequalities:*

$$\alpha \geq \xi, \ \beta \geq \xi,$$

for all $i \in \mathcal{N}$, and all $(i,j) \in \mathcal{E}$, where

$$\xi = 2 \max_{i \in \mathcal{N}^{(T)}} \left\{ -r_i[k] + \overline{p}_i - p_i^0[k], r_i[k] - \underline{p}_i + p_i^0[k] \right\} .$$

Then, (34)-(47) converge to an optimal solution of $\mathbf{M}_1^{(r)}$.

Theorem 1 enables us to select the values of the parameters $\underline{\alpha}_i$, $\overline{\alpha}_i$, $\underline{\alpha}_{i,j}$, $\overline{\alpha}_{i,j}$, and β_i such that the proposed control laws converge to an optimal solution of $\mathbf{M}_1^{(r)}$. Note that the proposed sufficient conditions on α and β are highly dependent on the values of $r_i[k]$'s and $p_i^0[k]$'s. The following result, the proof of which is provided in the appendix, enables us to select the values of the parameters α and β irrespective of the values of the signals $r_i[k]$'s and $p_i^0[k]$'s.

Corollary 1. *Given $\underline{r}_i$'s, $\overline{r}_i$'s, $p_i^0[k]$'s, $\underline{p}_i$'s, and $\overline{p}_i$'s, let $\alpha = \underline{\alpha}_{i,j} = \overline{\alpha}_{i,j} = \underline{\alpha}_i = \overline{\alpha}_i$, and $\beta = \beta_i$ be constants satisfying the following inequalities:*

$$\alpha \geq \xi, \ \beta \geq \xi,$$

for all $i \in \mathcal{N}$, and all $(i,j) \in \mathcal{E}$, where

$$\xi = 2 \max_{i \in \mathcal{N}^{(T)}} \left\{ -\underline{r}_i + \overline{p}_i - \underline{p}_i, \overline{r}_i + \overline{p}_i - \underline{p}_i \right\} .$$

Then, the set of control laws in (34)-(47) converge to an optimal solution of $\mathbf{M}_1^{(r)}$ irrespective of the values of $r_i[k]$'s and $p_i^0[k]$'s.

To determine the values of the design parameters, the microgrid operator only needs to know the values of $\overline{r}_i$'s, $\underline{r}_i$'s, $\overline{p}_i$'s, and $\underline{p}_i$'s which are constant over the contract duration $D = KT$, i.e., the microgrid only needs to configure its DERs at the beginning of each contract.

Let $f^\star(t_f)$, $g^\star(t_f)$, $\ell^\star(t_f)$, and $\Delta p^\star(t_f)$ denote the optimal values of our control variables, computed by the proposed control laws at time instant $t_f = (k+W-1)T$. The optimal values $f^\star(t_f)$, $g^\star(t_f)$, $\ell^\star(t_f)$, and $\Delta p^\star(t_f)$ will be the initial values of our control variables at time slot $(k+W)$. Recall that the ISO sends regulation signals every W time slots, and that given a new regulation signal, the microgrid operator needs to solve $\mathbf{M}_1^{(r)}$. Theorem 1 guarantees the convergence of the proposed control laws to an optimal solution of $\mathbf{M}_1^{(r)}$ irrespective of the initial values of the control variables. However, it does not guarantee that the trajectory, generated by the control laws, will always satisfy the physical constraints in (17)-(21) and (31) (especially at the beginning of each time slot $k \in \mathcal{K}$). The following result provides the conditions under which the trajectory will always satisfy the physical constraints in (17)-(21) and (31). The proof is provided in the appendix.

Proposition 1. *Let the optimal values of our control variables at time instant $t_f = (k-1)T$ satisfy*

$$(f^\star(t_f), g^\star(t_f), \ell^\star(t_f), \Delta p^\star(t_f)) \in \mathcal{F}_1^{(r)}[k],$$

where $\mathcal{F}_1^{(r)}[k]$ denotes the feasible set of problem $\boldsymbol{M}_1^{(r)}$ at time slot $k \in \mathcal{K}$. Then, the trajectory, generated by the control laws in (34)-(47), will satisfy the constraints (17)-(21) and (31) at all times during the time period $[(k-1)T, (k+W-1)T]$.

Proposition 1 shows that the trajectory will satisfy the physical constraints at all times during the time period $[(k-1)T, (k+W-1)T]$ if the initial values of our control variables at time slot $k \in \mathcal{K}$ form a set of feasible flows for the system. Therefore, we can obtain a set of feasible trajectories for the system (one for each time period $[(k-1)T, (k+W-1)T]$ where $k \in \mathcal{K}$) if the optimal solution of each time period $[(k-1)T, (k+W-1)T]$ is a feasible solution for the system at time slot $(k+W)$; otherwise, there will be an imbalance between demand and supply in the system. A careful selection of the upper and lower bounds on $g_i(t)$'s and $\ell_i(t)$'s allows us to avoid any imbalance in the system. The selection of the upper and lower bounds on $g_i(t)$'s and $\ell_i(t)$'s is out of the scope of this paper.

VI. Discretization of Control Laws

In practice, the proposed control laws have to be implemented in a discrete-time fashion over the cyber layer used to transmit feedback information among neighboring nodes. We propose a discrete-time approximation of the proposed continuous-time control laws in (34)-(47). Difference equations can be obtained from the differential equations in (34)-(47) in several ways. We use the forward rule approximation since it avoids computational delays inherent to other discretization techniques (e.g., trapezoidal or backward rule approximation). Note that we are considering only fast-following resources. Hence, we can ignore the fast time-scale dynamics of the DERs, and discretize (34), (39), (45), and (42) as follows:

$$g_i[k+1] = g_i[k] + s_0\bigg(\underline{\alpha}_i \underline{u}_i^{(g)}[k] - \overline{\alpha}_i \overline{u}_i^{(g)}[k] - \beta_i u_i[k]\bigg), \quad \forall i \in \mathcal{N}^{(G)}, \quad (48)$$

$$\ell_i[k+1] = \ell_i[k] + s_0\bigg(\underline{\alpha}_i \underline{u}_i^{(\ell)}[k] - \overline{\alpha}_i \overline{u}_i^{(\ell)}[k] + \beta_i u_i[k]\bigg), \quad \forall i \in \mathcal{N}^{(L)}, \quad (49)$$

$$f_a[k+1] = f_a[k] + s_0\bigg(\underline{\alpha}_{i,j} \underline{u}_{i,j}[k] - \overline{\alpha}_{i,j} \overline{u}_{i,j}[k] + \beta_i u_i[k] - \beta_j u_j[k]\bigg), \quad \forall e_a \in \mathcal{E}, \quad (50)$$

$$\Delta p_i[k+1] = \Delta p_i[k] + s_0\bigg(-2\left(\Delta p_i[k] - r_i[k]\right) + \underline{\alpha}_{i,j} \underline{u}_{i,j}[k] - \overline{\alpha}_{i,j} \overline{u}_{i,j}[k] + \beta_i u_i[k]\bigg), \quad \forall i \in \mathcal{N}^{(T)}, \quad (51)$$

where s_0 is the step size. The sliding mode control theory used in the proof of Theorem 1 cannot be applied to analyzing the convergence of (48), (49), (50), and (51). The following result shows that the discretized version of the control laws in (48), (49), (50), and (51) can realize a discrete-time version of our continuous-time control laws if the step size s_0 is chosen carefully and is small enough. The proof closely follows the one in [32, Result 2, p. 95].

Proposition 2. *Let $f(t)$, $g(t)$, $\ell(t)$, and $\Delta p(t)$ denote the trajectory obtained by our control laws in* (34), (39), (42), *and* (45), *and let $f[k]$, $g[k]$, $\ell[k]$, and $\Delta p[k]$ be the corresponding discrete-time trajectory computed by the laws in* (48), (49), (50), *and* (51). *Given any time interval $[t_1, t_2]$ and $\kappa > 0$, there exists $s_0 > 0$ such that*

$$||x(kT) - x[k]|| < \kappa$$

where $x(t) = [g(t)^{\mathrm{T}}, \ell(t)^{\mathrm{T}}, f(t)^{\mathrm{T}}, \Delta p(t)^{\mathrm{T}}]^{\mathrm{T}}$ and $x[k] = [g[k]^{\mathrm{T}}, \ell[k]^{\mathrm{T}}, f[k]^{\mathrm{T}}, \Delta p[k]^{\mathrm{T}}]^{\mathrm{T}}$.

Our discrete-time control laws will successfully follow their continuous-time counterpart if the step size s_0 is sufficiently small. Next, we numerically demonstrate the effectiveness of our discrete-time control laws.

VII. Numerical Results

We consider a microgrid consisting of three generator buses (buses 3, 6, and 9), 29 load buses (buses 1-2, 4-5, 7, 8, and 10-33), and one tie-line bus. The topology of this microgrid is shown in Fig. 2, a modified IEEE 33-bus distribution system from [33]. We take the generator parameters to be $\underline{g}_i = 0$ and $\overline{g}_i = 1$ pu $i = 3, 6, 9$, and assume that the loads are not controllable. The buses are connected via electrical transmission lines. The microgird is connected to the grid via the tie-line connected to bus 25. We take the thermal limits of the transmission lines and the tie-line to be equal to 0.8 pu, and assume that voltage magnitudes $V_i[k]$'s are constant and equal to 1 pu for all k and $i = 1, \cdots, 33$.

The major sources of delays in our algorithm arise from communication and computation tasks. To account for these sources of delays when evaluating the performance of our control laws, we select the time slot duration to be equal to 20 milliseconds, and assume that the cyber layer can transmit the feedback information among neighbors every 20 millisecond. This is consistent with the results in [34] where the authors built a testbed for microgrid distributed control, and showed that different nodes can successfully exchange their feedback information every 20 millisecond.

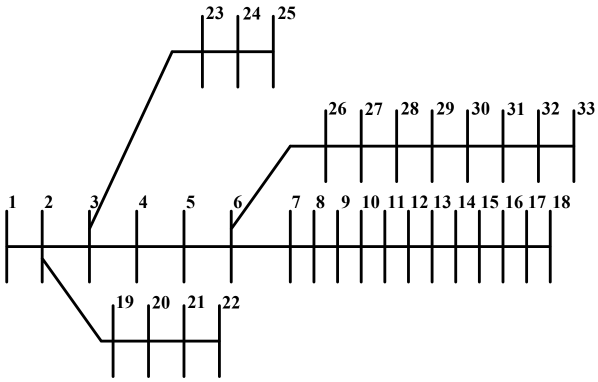

Fig. 2. A grid-connected microgrid comprising three generator buses, 29 load buses, and one tie-line bus.

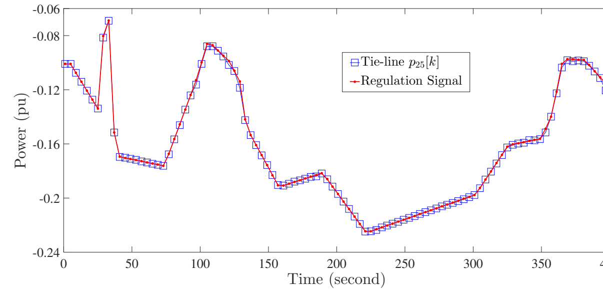

Fig. 3. Power exchange $p_{25}[k]$ and regulation signal $r[k]$ as a function of time.

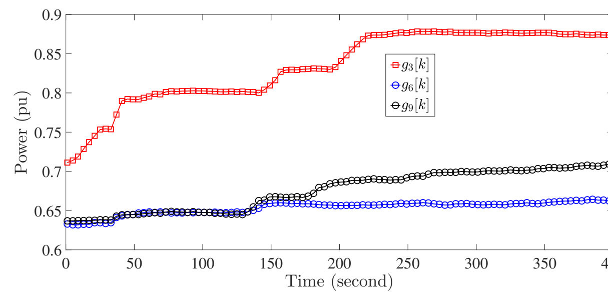

Fig. 4. The output of the DERs $g_3[k]$, $g_6[k]$, and $g_9[k]$ as a function of time.

We now focus on one single contract of duration $D = 1$ h, and assume that the ISO sends regulation signals to the microgrid every 4 s, i.e., a constant regulation demand is applied for each period of 4 s. This is consistent with automatic generation control signals (in practice, regulation signals are sent every 2 to 4 s [28]). The microgrid operator selects the values of its parameters to be $p_{25}^0 = 0$ and $\overline{r} = -\underline{r} = 0.3$ pu, and offers regulation services to the grid. As mentioned earlier, the computation of the parameters p_{25}^0, $\underline{r}$, and $\overline{r}$ is beyond the scope of this paper. Here, we assume that the values of these parameters are computed beforehand by the microgrid operator. Without loss of generality, we assume that the ISO accepts these parameters.

To demonstrate the effectiveness of our control laws, we consider a sequence of regulation signal values obtained from the PJM website for their so-called RegD signal for December 2016 [35]; see Fig. 3. Also, for brevity, we only show the results for a time period of length 400 s. Notice that we scale the regulation signal values to be in the interval $[\underline{r}, \overline{r}]$. We use our discrete-time control laws with the design parameters $\alpha = 20$ and $\beta = 20$ to compute the optimal set-points of the DERs as well as the optimal power flows over the lines. Note that we compute the optimal power flows over the lines in order to compute the feedback information for our control schemes. Our numerical results are shown in Figs. 3-5. The results show that our discrete-time control laws converge to an optimal solution to $\mathbf{M}_1^{(r)}$ in a short period of time without any oscillations. In addition, our numerical results show that communication and computational delays will not degrade the microgrid performance in the sense of providing the requested regulation service in practice.

VIII. Conclusion

In this paper, we focus on the optimal operation of grid-connected microgrids in frequency regulation markets, and formulate a joint DER scheduling and power flow optimization problem. Our goal is to optimize the injections of the DERs and the power flows over the lines in a distributed fashion; to do so, we follow three steps. We first focus on the feasibility set of the DER scheduling problem, and relax the non-convex feasible set. Then, we obtain a convex relaxation of the DER scheduling problem. In the second step, we propose a set of decentralized control laws that converge to an optimal solution of the relaxed problem. We prove that our control laws result in feasible power flows and injections for the system at each time instant. Finally, we discretize the proposed control laws, and numerically demonstrate their effectiveness. One possible direction for future research is the microgrids with non-uniform resistance-to-reactance ratios.

Appendix

In this appendix, we provide the proofs of Theorem 1 and Proposition 1.

Proof of Theorem 1

Let us begin with introducing some notation that allows us to simplify the exposition to follow. Without loss of generality, problem $\mathbf{M}_1^{(r)}$ can be represented in the following form:

$$\mathbf{M}_1^{(r)} : \min_{x} f(x)$$

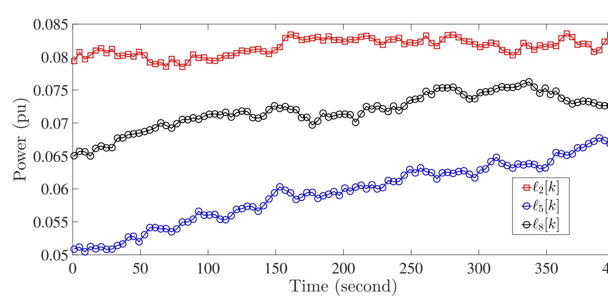

Fig. 5. The output of the DERs $\ell_2[k]$, $\ell_5[k]$, and $\ell_8[k]$ as a function of time.

$$\text{s.t} \ \ h_i(x) \leq 0, \ i = 1, \cdots, \psi,$$
$$h_i(x) = 0, \ i = \psi + 1, \cdots, \Psi,$$

where $f(x)$ is a convex differentiable function and $h_i(x)$'s are affine functions for all i.

Given the form of the constraints and objective function in $\mathbf{M}_1^{(r)}$, the control laws can be represented by

$$\dot{x} = -\nabla f(x) - G(x)u, \tag{52}$$

where $\nabla f(x)$ denotes the gradient of $f(x)$, $u = [u_1, \cdots, u_\Psi]^{\mathrm{T}}$ is an Ψ-dimensional vector, and $G(x)$ is the following matrix

$$G(x) \doteq [\nabla h_1(x) \cdots \nabla h_\Psi(x)] \ .$$

For $i = 1, \cdots, \psi$, the entries of u are of the form

$$u_i = \begin{cases} \nu_i, \ \text{if } h_i > 0, \\ 0, \ \text{if } h_i < 0, \end{cases} \tag{53}$$

where $\nu_i = \underline{\alpha}_i$ for the lower bounds on $p_i[k]$'s, $\ell_i[k]$'s, and $g_i[k]$'s in (19)-(21), $\nu_i = \overline{\alpha}_i$ for the upper bounds on $p_i[k]$'s, $\ell_i[k]$'s, and $g_i[k]$'s in (19)-(21), $\nu_i = \underline{\alpha}_{i,j}$ for the lower bounds on $f_a[k]$'s in (31), and $\nu_i = \overline{\alpha}_{i,j}$ for the upper bounds on $f_a[k]$'s in (31). For $i = \psi + 1, \cdots, \Psi$, the entries of u are of the form

$$u_i = \begin{cases} \eta_i, \ \text{if } h_i > 0, \\ -\eta_i, \ \text{if } h_i < 0, \end{cases} \tag{54}$$

where $\eta_i = \beta_i$ for the flow conservation constraints in (17) and (18). To show that the control laws in (52) converge to the optimal value of $f(x)$ in $\mathbf{M}_1^{(r)}$ from any initial condition, we need two steps:

Step 1: Let us define function $\widehat{F}(x)$ as follows:

$$\widehat{F}(x) \doteq f(x) + H(x),$$

where $H(x) = [h_1(x) \cdots h_\Psi(x)]^{\mathrm{T}} u$. The following results show that the trajectories generated by the control laws converge to the minimum of the function $\widehat{F}(x)$ from any initial condition. For the proofs of Lemmas 1-4, we refer the reader to [31].

Lemma 1. *The function $\widehat{F}(x)$ does not increase along the trajectories.*

Lemma 2. *The time derivative of $\widehat{F}(x)$ is zero only when $\dot{x} = 0$.*

Lemma 3. *The stationary points of $\widehat{F}(x)$ are the minimum points of $\widehat{F}(x)$.*

Lemma 4. *If the set of all minimum points of $\widehat{F}(x)$ is bounded, then the control laws in (52) will converge to this set from any initial condition.*

Step 2: We now need to show that the minimum of $\widehat{F}(x)$ coincides with the minimum of $f(x)$. The following result provides the necessary and sufficient conditions under which the minimum of $\widehat{F}(x)$ coincides with the minimum of $f(x)$.

Theorem 2. *[31] Let $\mathbf{u}$ be a vector whose entries are of the form*

$$0 \leq \mathbf{u}_i \leq \nu_i, \ i = 1, \cdots, \psi,$$
$$-\eta_i \leq \mathbf{u}_i \leq \eta_i, \ i = \psi + 1, \cdots, \Psi,$$

where $\mathbf{u}_i = 0$ for nonbinding constraints. Then, the minimum of $\widehat{F}(x)$ coincides with the minimum of the function $f(x^\star)$ if and only if there exists $x^\star$ such that

$$\nabla f(x^\star) = -G(x^\star)\mathbf{u} \ .$$

The proposed conditions on the design parameters $\underline{\alpha}_i$, $\overline{\alpha}_i$, $\underline{\alpha}_{i,j}$, $\overline{\alpha}_{i,j}$, and β_i in Theorem 1 ensure that the necessary and sufficient conditions of Theorem 2 are satisfied for problem $\mathbf{M}_1^{(r)}$. Let us select an arbitrary generator or load bus $i_1 \in \mathcal{N}^{(G)} \cup \mathcal{N}^{(L)}$ and an arbitrary tie-line bus $i_2 \in \mathcal{N}^{(T)}$, and a directed path from bus i_1 to bus i_2. Note that such a path exists since graph $\mathcal{G}(\mathcal{N}, \mathcal{E})$ is connected. Without loss of generality, let us assume that $i_1 \in \mathcal{N}^{(G)}$. Now, summing the rows in $\nabla f(x^\star) = -G(x^\star)\mathbf{u}$ associated with the edges along the path, we obtain

$$\left(\mathbf{1}_{i_1 \in \mathcal{N}^{(G)}} - \mathbf{1}_{i_1 \in \mathcal{N}^{(L)}}\right)\left(\underline{\mathbf{u}}_{i_1}^{(g)} - \overline{\mathbf{u}}_{i_1}^{(g)}\right) + \underline{\mathbf{u}}_{i_2,j_2} - \overline{\mathbf{u}}_{i_2,j_2} + \sum_{(i,j)\in\mathcal{P}_{i_1,i_2}} \lambda_{i,j}(\underline{\mathbf{u}}_{i,j} - \overline{\mathbf{u}}_{i,j}) = 2\left(\Delta p_{i_2}^\star - r_{i_2}\right), \tag{55}$$

where (i_2, j_2) and $\mathcal{P}_{i_1,i_2}$ denote the tie-line connected to bus i_2 and the set of edges along the path, respectively. $\lambda_{i,j}$ is equal to (-1) if edge (i,j) and path $(i_1, \cdots, i_2, j_2)$ do not have the same direction; otherwise, it is one. Then, the worst case value of $\mathbf{u}_i$ for all $i = 1, \cdots, \psi$ equals ξ where

$$\xi = 2 \max_{i \in \mathcal{N}^{(T)}} \left\{-r_i[k] + \overline{p}_i - p_i^0[k], r_i[k] - \underline{p}_i + p_i^0[k]\right\} \ .$$

Therefore, the worst case value of $\mathbf{u}_i$ associated with the inequality constraints will be equal to ξ. We now use this information to compute the worst case values of the other entries of $\mathbf{u}$. Note that these entries are associated with the flow conservation constraints in $\mathbf{M}_1^{(r)}$. By using the control laws in (34), (39), and (42), we can verify that the worst case value of the entries of $\mathbf{u}$ associated with the flow conservation constraints equals ξ. To satisfy the conditions of Theorem 2, we need to have

$$\mathbf{u}_i \leq \xi < \nu_i, \ i = 1, \cdots, \psi,$$
$$|\mathbf{u}_i| \leq \xi < \eta_i, \ i = \psi + 1, \cdots, \Psi \ .$$

Therefore, the proposed control laws converge to the optimal value of $\mathbf{M}_1^{(r)}$ after finite time. This completes the proof.

Proof of Proposition 1

At time instant $t_f = (k-1)T$, the optimal values of our decision variables satisfy $(f^\star(t_f), g^\star(t_f), \ell^\star(t_f), \Delta p^\star(t_f)) \in \mathcal{F}_1^{(r)}[k]$. Therefore, at the beginning of time slot k, the initial values of the decision variables form a feasible solution to $\mathbf{M}_1^{(r)}$, and the trajectory starts from a point inside the feasibility region of $\mathbf{M}_1^{(r)}$. Let us assume that the trajectory hits the boundary of the feasible region $\mathcal{F}_1^{(r)}[k]$ at $t = t_0$ ($t_f \leq t_0$), and leaves the feasible region $\mathcal{F}_1^{(r)}[k]$ at $t = t_1$ where $t_f \leq t_0 < t_1$. Using the definition of penalty function, we will have $\widehat{F}(x(t_0)) \leq \widehat{F}(x(t_1))$ since $x(t_1)$ is outside the feasibility region $\mathcal{F}_1^{(r)}[k]$. This contradicts with the fact that $\widehat{F}(x)$ does not increase along the trajectory (see Lemma 1).

Hence, the trajectory will stay in the feasibility region $\mathcal{F}_1^{(r)}[k]$ at all times during the time period $[(k-1)T, (k+W-1)T]$. This completes the proof.

References

[1] R. Lesseter, “MicroGrids,” *in IEEE Power Engineering Society Winter Meeting*, vol. 1, pp. 305--308, 2002.

[2] N. Hatziagyriou, H. Asano, R. Iravani, and C. Marnay, “Microgrids,” *IEEE Power and Energy Magazine*, vol. 5, no. 4, pp. 78–94, 2007.

[3] G. Strbac, N. Hatziargyriou, J. P. Lopes, C. Moreira, A. Dimeas, and D. Papadaskalopoulos, “Microgrids: Enhancing the resilience of the European megagrid,” *IEEE Power and Energy Magazine*, vol. 14, no. 3, pp. 35--43, 2015.

[4] F. Katiraei, R. Iravani, N. Hatziargyriou, and A. Dimeas, “Microgrids management,” *IEEE Power Energy Magazine*, vol. 6, no. 3, pp. 54–65, May 2008.

[5] A. G. Tsikalakis, and N. D. Hatziargyriou, “Centralized control for optimizing microgrids operation,” *IEEE Trans. Energy Convers.*, vol. 23, no. 1, pp. 241–248, Mar. 2008.

[6] M. Smith, and D. Ton, “Key Connections: the U.S. Department of Energy’s microgrid initiative,” *IEEE Power and Energy Magazine*, vol. 11, no. 4, pp. 22–27, 2013.

[7] J. A. P. Lopes, C. L. Moreira, and A. G. Madureira, “Defining control strategies for MicroGrids islanded operation,” *IEEE Trans. Power Syst.*, vol. 21, no. 2, pp. 916–924, May 2006.

[8] S. Parhizi, H. Lotfi, A. Khodaei, and S. Bahramirad, “State of the Art in Research on Microgrids: A Review,” in *IEEE Access*, vol. 3, no. , pp. 890–925, 2015.

[9] M. Yazdanian, and A. Mehrizi-Sani, “Distributed Control Techniques in Microgrids,” in *IEEE Transactions on Smart Grid*, vol. 5, no. 6, pp. 2901–2909, Nov. 2014.

[10] F. Katiraei, and M. R. Iravani, “Power management strategies for a microgrid with multiple distributed generation units,” *IEEE Trans. Power Syst.*, vol. 21, no. 4, pp. 1821–1831, Nov. 2006.

[11] R. Majumder, A. Ghosh, G. Ledwich, and F. Zare, “Power management and power flow control with back-to-back converters in a utility connected microgrid,” *IEEE Trans. Power Syst.*, vol. 25, no. 2, pp. 821–834, May 2010.

[12] A. Mehrizi-Sani, and R. Iravani, “Potential-function based control of a microgrid in islanded and grid-connected modes,” *IEEE Trans. Power Syst.*, vol. 25, no. 4, pp. 1883–1891, Nov. 2010.

[13] C. L. Moreira, F. O. Resende, and J. A. P. Lopes, “Using low voltage MicroGrids for service restoration,” *IEEE Trans. Power Syst.*, vol. 22, no. 1, pp. 395–403, Feb. 2010.

[14] G. Diaz, C. Gonzalez-Moran, J. Gomez-Aleixandre, and A. Diez, “Scheduling of droop coefficients for frequency and voltage regulation in isolated microgrids,” *IEEE Trans. Power Syst.*, vol. 25, no. 1, pp. 489–496, Feb. 2010.

[15] Microgrid at Illinois Institute of Technology. [Online]. Available: http://www.iitmicrogrid.net/.

[16] N. Hatziargyriou, “The more microgrids project,” *in Smart Electricity Networks, retrieved from Demonstration of Smart Distribution Network Solutions, Contractors Meeting*, Brussels, 2009. Available: https://ec.europa.eu/research/conferences/2009/smartnetworks/pdf/microgrids.pdf.

[17] M. D. Ilic, “From hierarchical to open access electric power systems,” *Proc. IEEE*, vol. 95, no. 5, pp. 1060–1084, May 2007.

[18] J. R. Winkelman, J. H. Chow, J. J. Allemong, and P. V. Kokotovic, “Multi-time-scale analysis of a power system,” *Automatica*, vol. 16, no. 1, pp. 35–43, Jan. 1980.

[19] S. Mizani and A. Yazdani, “Optimal design and operation of a grid-connected microgrid,” *IEEE Electrical Power & Energy Conference*, pp. 1–6, Montreal, QC, 2009.

[20] Q. Jiang, M. Xue, and G. Geng, “Energy Management of Microgrid in Grid-Connected and Stand-Alone Modes,” in *IEEE Trans. on Power Systems*, vol. 28, no. 3, pp. 3380–3389, Aug. 2013.

[21] P. Malysz, S. Sirouspour and A. Emadi, “An Optimal Energy Storage Control Strategy for Grid-connected Microgrids,” in *IEEE Trans. on Smart Grid*, vol. 5, no. 4, pp. 1785–1796, July 2014.

[22] A. C. Luna, N. L. Diaz, M. Graells, J. C. Vasquez, and J. M. Guerrero, “Online energy management system for distributed generators in a grid-connected microgrid,” *IEEE Energy Conversion Congress and Exposition*, pp. 4616–4623, Montreal, QC, 2015.

[23] Z. Wang, W. Wu, and B. Zhang, “A fully distributed active power control method with minimum generation cost in grid-connected microgrids,” *IEEE Power & Energy Society General Meeting*, pp. 1–5, Denver 2015.

[24] V. Yadav, and M. V. Salapaka, “Distributed protocol for determining when averaging consensus is reached,” *45th Annual Allerton Conference*, pp. 715–720, 2007.

[25] M. Zholbaryssov, and A. D. Domínguez-García, “Exploiting Phase Cohesiveness for Frequency Control of Islanded Inverter-Based Microgrids,” *IEEE, Trans. on Control of Network Systems*, accepted for publication.

[26] H. Zhou, C. A. Hans, and W. Zhang, “Minimax model predictive operation control of grid-connected microgrids,” *IEEE Conference on Control Applications*, pp. 58–63, Buenos Aires, 2016.

[27] S. Seshu and M. B. Reed, *Linear Graphs And Electrical Networks*. Addison-Wesley, 1961.

[28] Performance, Mileage and the Mileage Ratio. [Online]. Available: http://www.pjm.com.

[29] L. Luo and S. Dhople, “Spatiotemporal model reduction of inverter-based islanded microgrids,” *IEEE Trans. Energy Conversion*, vol. 29, no. 4, pp. 823–832, 2014.

[30] F. Dorfler, J. Simpson-Porco, and F. Bullo, “Breaking the hierarchy: Distributed control and economic optimality in microgrids,” *IEEE Trans. Control Network Syst.*, vol. 3, no. 3, pp. 241–253, 2016.

[31] V. I. Utkin, *Sliding Modes in Control and Optimization.*, ser. Communications and Control Engineering Series, Berlin, Germany: Spriger-Verlag, 1992, vol. 66.

[32] A. F. Filippov, *Differential Equations with Discontinuous Righthand Sides*, ser. Mathematics and Its Applications. Dordrecht, The Netherlands: Kluwer, 1988.

[33] M. E. Baran, and F. F. Wu, “Network reconfiguration in distribution systems for loss reduction and load balancing,” *in IEEE Transactions on Power Delivery*, vol. 4, no. 2, pp. 1401–1407, Apr 1989.

[34] S. T. Cady, A. D. Domínguez-García, and C. N. Hadjicostis, “A Distributed Generation Control Architecture for Islanded AC Microgrids,” *in IEEE Transactions on Control Systems Technology*, vol. 23, no. 5, pp. 1717–1735, Sept. 2015.

[35] RTO, Regulation Signal Data. [Online]. Available: http://www.pjm.com/markets-and-operations/ancillary-services.aspx.

Dariush Fooladivanda received the Ph.D. degree from the University of Waterloo, in 2014, and a B.S. degree from the Isfahan University of Technology, all in electrical engineering. He is currently a Post-doctoral Research Associate in the Department of Electrical and Computer Engineering at the University of Illinois at Urbana-Champaign. His research interests include theory and applications of control and optimization in large scale networked systems.

Madi Zholbaryssov (S’16) received the B.S. degree in electrical engineering in 2011 and the M.S. degree in electrical engineering in 2014, both from the University of Illinois at Urbana-Champaign, Urbana, IL, USA, where he is currently pursuing the Ph.D.degree in electrical engineering.

His current research interests include distributed control, distributed optimization and their application to electric power systems.

Alejandro D. Domínguez-García (S'02, M'07) received the degree of Electrical Engineer from the University of Oviedo (Spain) in 2001 and the Ph.D. degree in electrical engineering and computer science from the Massachusetts Institute of Technology, Cambridge, MA, in 2007.

He is an Associate Professor with the Department of Electrical and Computer Engineering (ECE), and a Research Associate Professor with the Coordinated Science Laboratory and the Information Trust Institute, all at the University of Illinois at Urbana-Champaign. He is affiliated with the ECE Power and Energy Systems area, and has been a Grainger Associate since August 2011.

His research interests are in the areas of system reliability theory and control, and their applications to electric power systems, power electronics, and embedded electronic systems for safety-critical/fault-tolerant aircraft, aerospace, and automotive applications.

Dr. Domínguez-García received the NSF CAREER Award in 2010, and the Young Engineer Award from the IEEE Power and Energy Society in 2012. In 2014, he was invited by the National Academy of Engineering to attend the US Frontiers of Engineering Symposium, and was selected by the University of Illinois at Urbana-Champaign Provost to receive a Distinguished Promotion Award. In 2015, he received the U of I College of Engineering Dean's Award for Excellence in Research. He is an editor of the IEEE Transactions on Power Systems and IEEE Power Engineering Letters.